Modelling bedload transport for mixed flows in presence of a non-erodible bed layer.

G. Corestein, E. Bladé & D. Niñerola
Institut Flumen (UPC-CIMNE), Universitat Politècnica de Catalunya – BarcelonaTech, Barcelona, Spain

ABSTRACT: Recently the number of 1D and 2D modelling tools that use the Finite Volume Method with upwind and explicit schemes aiming to solve the SWE together with sediment transport has progressively increased. This work focuses on two issues that arise when extending a numerical code initially designed for water flow to include bedload sediment transport: the upwinding of the sediment fluxes, and how to deal with a non-erodible layer. For both of them simple but effective methods are presented. The Roe scheme is implemented for the SWE and a first order one-sided scheme for the sediment continuity equation. In contrast to other approaches, to deal with the non-erodible layer a predictor – corrector method is used for the computation of bedload fluxes. The procedures are validated using existing standard benchmarks. Also a new test case of a channel with transcritical flow and erodible and non-erodible reaches is presented.

1 INTRODUCTION

There are quite a lot numerical models that allow simulating bedload transport based on solving the Saint Venant plus Exner equations and any of the solid discharge formulas available from literature. Whether speaking of an academic model or about a commercial model it generally happens that, apart from basic information such as the equations to be solved and the numerical scheme, there is a lack of information on other aspects related with the implementation that may lead to complications when writing a code. This work aims to present some details of an implementation of bedload transport, using the Finite Volume Method (FVM), into a numerical model. The proposed model is suitable to be applied to subcritical, supercritical and transcritical regimes. The focus will be placed on:

- The importance of an appropriate upwinding strategy of the bedload numerical terms
- A strategy to deal with the presence of a non-erodible layer, or rock layer.

To deal with the first of the previous points, the hyperbolic character of the complete system of equations is considered, but the solution of water and sediment flows is done in an uncoupled way using a Roe type scheme. The alternative of using the whole system of equations, and thus working with the full system Jacobian matrix, its eigenvectors and eigenvalues, is deliberately avoided. This option is the one proposed by other authors as Benkhaldoun *et al.* (2009), Benkhaldoun *et al.* (2013), Castro Díaz *et al.* (2009), Serrano-Pacheco *et al.* (2012). Instead of this, what is proposed here is the application of the scheme of Roe for water conservation and momentum equations and a simple upwind scheme for bedload transport. This strategy makes the addition of a sediment transport module to an existing hydrodynamic model to be relatively easy and direct. Moreover it enables to straightforwardly use any of the many sediment transport formula available such as Meyer-Peter&Müller, Van Rijn, etc., which are widely used in the engineering field, while schemes based on the Jacobian matrix of the whole system usually end up using the simple Grass formula, (Grass 1981) due to the complexity of deriving eigenvectors and eigenvalues for other formulas. Practical aspects of its numerical implementation are presented along this work.

This proposed methodology is tested and validated satisfactorily using some benchmarks available in bibliography such as the conical dune evolution proposed originally by De Vriend (1987) and recently used by Hudson (2001).

There is limited information on the literature regarding the details of the numerical methods used to deal with a non-erodible layer. The method presented by Struiksma (1999) considers a correction of the solid discharge in the Exner equation with good results for erosion and sedimentation but needs some corrections when the value of the solid discharge is needed. Hervouet *et al.* (2003) presented the details of a method when using the Finite Element Method. More recently, Rulot & Dewals (2012) present an al-

ternative iterative method: the flux minimization method. In this paper a predictor-corrector approach is presented to be used with the FVM. Like the flux minimization method, it is based on the correction of the fluxes when computed sediment level is below the rigid bottom, but no iterations are needed. As most FVM for 2D-SWE are explicit and use very small time steps, coupling them to an iterative method for sediments can be computationally expensive. In the two-steps proposed method, bedload capacity is used in the first step, while for the second one the solid discharge fluxes are corrected if the rock layer elevation is reached.
Summarizing, this communication focuses in two concrete but key aspects of the numerical implementation of bedload sediment transport, which are solved using simple but very effective methods, as the validation tests show.

2 EQUATIONS

The developments presented in this section are part of the sediment transport module of Iber . Iber is a two dimensional river modelling tool which solves the 2D Saint Venant equations, or 2D-SWE, with a Roe type scheme based on the FVM.

The sediment transport module calculates the bed load and suspended transport adding the Exner expression for sediment mass conservation:

$$(1-p)\frac{\partial Z_b}{\partial t}+\frac{\partial q_{sb,x}}{\partial x}+\frac{\partial q_{sb,y}}{\partial y}=D-E \qquad (1)$$

where p = sediment porosity, Z_b = bed load elevation, $q_{sb,x}$ = x-component of sediment discharge and y $q_{sb,y}$ = y-component of sediment discharge. The difference D - E works as a coupling term that represents a balance between bed load and suspended load. This article focuses just in bedload, thus D and E are considered zero.

As is well known the sediment discharge referred in Equation (1) can be estimated using empirical expressions. At the present version, two of the most know and accepted formulas are implemented in the code: Meyer-Peter & Müller (Wong and Parker 2006) and Van Rijn (van Rijn 1984).

The expression for Meyer-Peter & Müller that has been used to evaluate the non-dimensional solid discharge in this work is one of the two proposed by Wong and Parker (Wong and Parker 2006), in particular the one that keeps the original exponent value:

$$q_{sb}^{*}=3.97(\tau_b^{*}-\tau_c^{*})^{3/2} \qquad (2)$$

τ_b^{*} = non-dimensional bed shear stress. For horizontal bottoms, when using the above mentioned expression, the value to use is τ_c^{*} = 0.0495. When this is not the case, a correction due the bottom slope is required.

3 NUMERICAL SCHEME

In the FVM the updating in time of the conserved variables in every finite volume, or mesh element, is performed by considering the balance of the fluxes across the mesh element edges. In this way, the discretization of the Exner equation can be written as:

$$z_i^{n+1}=z_i^{n}-\frac{\Delta t}{(1-\lambda)V_i}\sum_{w=1}^{N_i}(\mathbf{q}_{s,w}\mathbf{n}_{i,w})l_{i,w} \qquad (3)$$

where z_i^{n} = elevation of element i at time step n, λ = the porosity, V_i = area of element i, N_i = number of edges of the element, $l_{i,w}$ = length of edge w of element i, $\mathbf{q}_{s,w}$ = solid discharge (vector) across the edge, and $\boldsymbol{n}_{s,w}$ = external normal unit vector for w edge.

3.1 *Upwinding of sediment fluxes*

One possibility to solve this point is to simply apply an upwind non-centred interpolation, as is generally used for the advection terms of transport equations as, for example, suspended sediment. This methodology is simple but problems of instabilities could appear due to differences between velocities of propagation of water and sediments. This complex phenomena is reported and commented by various authors (Castro Díaz *et al.* 2009, Murillo & García-Navarro 2010).
Struiksma derivate an expression for bed perturbation celerity (Struiksma 1999).

$$c=\frac{1}{1-Fr^2}\psi\frac{u}{h}\frac{\partial S_f}{\partial u}+\frac{S_f}{\delta_a}\frac{\partial\psi}{\partial(\delta/\delta_a)}\left(1+\frac{1}{1-Fr^2}\frac{\delta}{\delta_a}\frac{\partial\delta_a}{\partial h}\right) \qquad (4)$$

where Fr = Froude number, ψ = correction factor , u = velocity, h = water depth, Sf = sediment discharge (volumetric) , δ = thickness of the non-erodible bed, δa = maximum thickness at what non-erodible bed affects sediment transport.

From this expression it could be inferred that the sign of the celerity change with Froude number.

Following that idea a simple implementation is proposed. The approach is to use a one-sided interpolation but applying upwind or downwind sense depending on Froude number value and water flux direction (Equation 4).

$$(\mathbf{q}_{sb})_{ij}=\mathrm{q}_{sb,i}\ \ if\begin{cases}((\mathbf{q}\cdot\mathbf{n})_{ij}>0\ and\ \mathrm{Fr}<1)\\ or\\ ((\mathbf{q}\cdot\mathbf{n})_{ij}<0\ and\ \mathrm{Fr}>1)\end{cases}$$

$$(\mathbf{q}_{sb})_{ij}=\mathrm{q}_{sb,j}\ \ if\begin{cases}((\mathbf{q}\cdot\mathbf{n})_{ij}<0\ and\ \mathrm{Fr}<1)\\ or\\ ((\mathbf{q}\cdot\mathbf{n})_{ij}>0\ and\ \mathrm{Fr}>1)\end{cases} \qquad (5)$$

$\mathbf{q}_{sb,ij}$ = sediment flux across edge *ij*, $\mathbf{q}_{sb,i}$ = sediment flux in element *i*, $\mathbf{q}$ = specific water discharge, $\mathbf{n}$ = edge *ij* normal and Fr = Froude number. The outline of the variables can be seen in Figure 1.

This simple procedure avoids the occurrence of the above mentioned instabilities, as is clearly shown in a practical example presented in section 4.2.

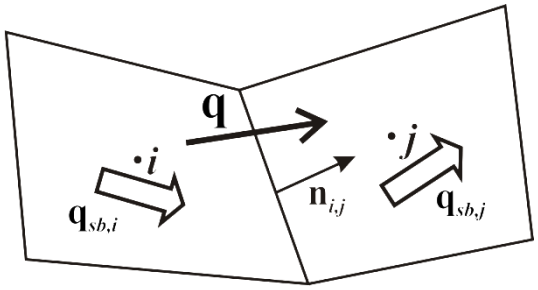

Figure 1: outline of sediment fluxes for one-sided scheme.

3.2 *Non-Erodible Layer*

Equation 3 applies only when a rock layer is not present or when this layer is not reached by the erosion process. As said in the introduction, if there is a non-erodible layer, the single step of equation (3) is decomposed in two: predictor and corrector. In the predictor step, a prediction of the final bottom level in every element, z_i^p is obtained considering only the outward fluxes:

$$z_i^p = z_i^n - \frac{\Delta t}{(1-\lambda_p)V_i}\sum_{i=1}^{N_i}\left(max\left(\mathbf{q}_{s,i,w}^n \mathbf{n}_{i,w}\right), \mathbf{0}\right) l_{i,w} \qquad (6)$$

After that, if this predicted bottom is below the rigid bottom, the outwards fluxes of sediment across the edges are corrected to ensure a final bed at the rock level position (Figure 2):

$$\text{If} \begin{Bmatrix} z_i^p < z_{rock} \\ \text{and} \\ \left(\mathbf{q}_{s,i,w}^n \mathbf{n}_{i,w}\right) > 0 \end{Bmatrix} \Rightarrow \begin{cases} \mathbf{q}_{s,i,w}^c = \frac{\mathbf{q}_{s,i,w}^n (z_i^n - z_{rock})}{(z_i^n - z_i^p)} \\ \mathbf{q}_{s,j,w}^c = -\mathbf{q}_{s,i,w}^n \end{cases} \qquad (7)$$

if not:

$$\mathbf{q}_{s,i,w}^c = \mathbf{q}_{s,i,w}^n \qquad (8)$$

$\boldsymbol{q}^c{}_{s,i,w}$ = corrected sediment flux at edge w of element *i*, and $\boldsymbol{q}^c{}_{s,j,w}$ = corrected flux for the same edge of the adjacent element *j* (Figure 3).

Figure 2: Predictor – corrector process.

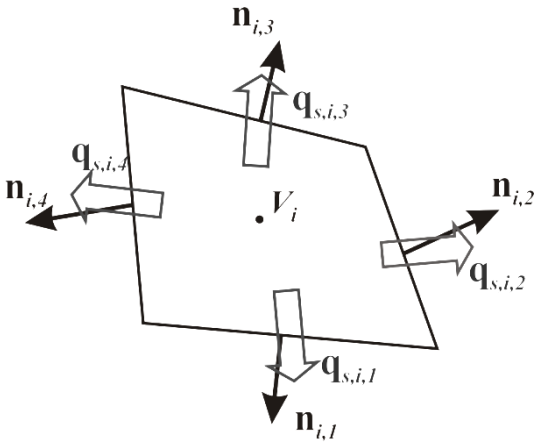

Figure 3: Sediment fluxes across element edges.

Finally, the corrected fluxes are used to update the bottom level:

$$z_i^{n+1} = z_i^n - \frac{\Delta t}{(1-\lambda_p)V_i}\sum_{i=1}^{N_i}\left(\mathbf{q}_{s,w_l}^c \mathbf{n}_{i,w_l}\right) l_{i,w_l} \qquad (9)$$

4 VALIDATION TESTS

4.1 *Conical Dune*

The above proposed methodology is tested and validated satisfactorily using an accepted benchmark such as the conical dune evolution proposed originally by De Vriend (1987) and more recently by Hudson (2001). This example is interesting and relevant because it is possible to know its exact solution. In this case what is expected is that the dune propagates into a star shaped dune with a specific spread angle.

The test problem consists of a channel of length 1000 m × 1000 m, with dummy initial conditions h(x, y, 0) = 10 − B(x, y, 0); u(x, y, 0) = Q / h(x, y, 0); v(x, y, 0) = 0 and the initial bathymetry is a conical sand dune (Figure 4),

$$B(x,y,0) = \begin{cases} \sin^2\left(\frac{\pi(x-300)}{200}\right)\sin^2\left(\frac{\pi(y-400)}{200}\right) & if\ 300 \le x \le 500, \\ & 400 \le y \le 600, \\ 0 & \text{otherwise} \end{cases} \qquad (10)$$

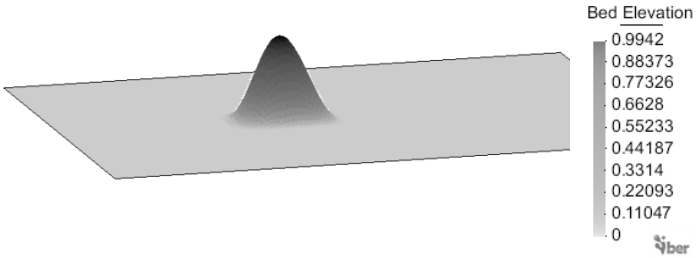

Figure 4: Initial bathymetry for conical sand dune benchmark.

In this case the sediment transport discharge is calculated using the Grass' formula (Grass 1981). This formula is a very simple relation expressed as:

$$q_{sb}^{*} = A_g |v| |v|^{m_g - 1} \qquad (11)$$

For the first simulation A_g=0.001 and m_g=3 are used. The values for the coefficients are selected based on the recommendations of the existent literature (Hudson 2001, Castro Díaz *et al.* 2009, Serrano-Pacheco *et al.* 2012).

The exact solution derived by De Vriend, when using Grass' formula, takes the following form (Hudson 2001)

$$\tan \alpha = \frac{3\sqrt{3}(m_g - 1)}{9 m_g - 1} \qquad (12)$$

using the recommended m_g=3 the expected angle of spread is:

$$\alpha = \tan^{-1}\left(\frac{3\sqrt{3}}{13}\right) = 21.7867893°$$

This solution applies only when interaction between water and sediment is slow. For the case of Grass' formula this means that $A_g < 0.01$.

Several runs with different meshes were performed. The results presented correspond to a domain discretized in a non-structured mesh of 35376 triangular volumes (mean side = 8 m).

After 100 h of simulation, a time proposed by De Vriend and used also in posterior references as Hudson 2001, Castro Díaz *et al.* 2009, Serrano-Pacheco *et al.* 2012, the initial conical dune moved and spread as expected. The initial dune evolves into a star shaped dune with an approximate angle of spread of 24.5º as is shown in Figure 5. A value that it is in the order of the ones achieved by the above mentioned authors.

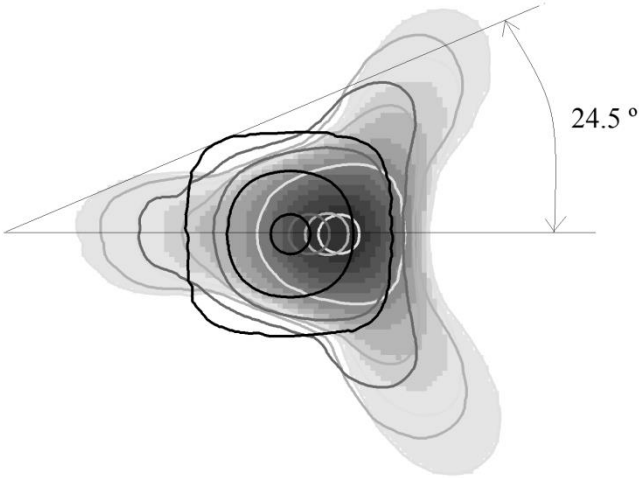

Figure 5: Approximate angle of spread of the conical dune.

The elevation of the top of the conical dune initially is 0.9942 m, as can be seen in Figure 4, after 100 h of simulation the dune travel downstream and the peak decrease in about a 10 % resulting in 0.90373 m (Figure 6).

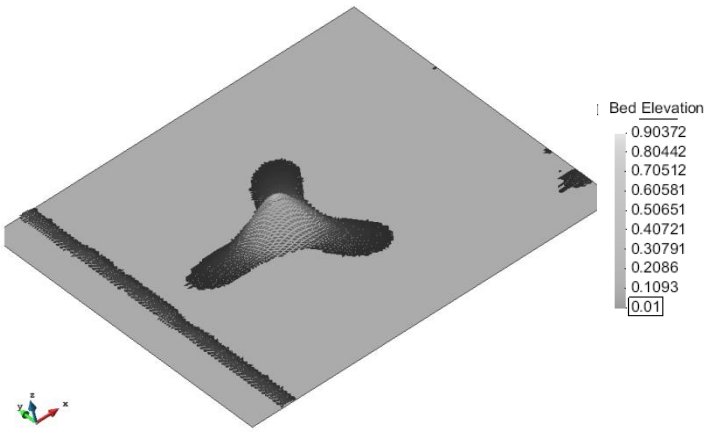

Figure 6: Bed evolution after 100 h for a slow interaction simulation

A second simulation is run considering high interaction between the two phases, water and sediment, thus using A_g=0.1 and maintaining the rest of the parameters. The evolution of the conical dune after 2 ½ h of simulation are shown in

Figure 7. Although the angle of spread cannot be calculated, equation 11 is not valid in the case of high interaction (Hudson 2001); the star shaped pattern is also reached. In this figure it also evident the no presence of instabilities in the results.

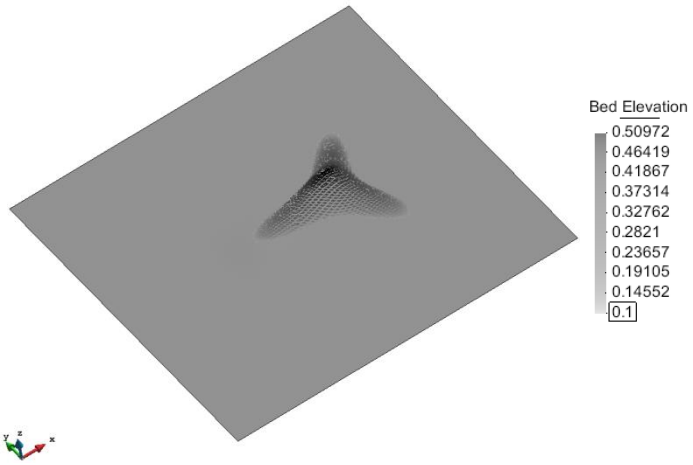

Figure 7: Bed evolution of 2 ½ h for high interaction simulation.

4.2 *Channel with sediment step*

In this case two different implementations are tested; the upwind option and the upwind & downwind proposed one.

This test consists of a channel of 15 m length, a cross section of 0.5 m x 0.5 m and 0.052 % slope. A layer of 4.5 cm of sand is placed in the central part of the channel, between 4.5 m and 9 m from the upstream end. Boundary conditions are: a constant discharge q = 0.022 m^3/s at the inlet and h= 0.115 m water depth at the outlet. A Manning coefficient n = 0.011, uniform sediment of 1 mm diameter and porosity of 0.4 are used.

The domain is discretized using a quadrilateral structured mesh of 1860 elements.

Figure **10** following figures show the results of bed elevation and Froude number for the two simulations, one with each of the proposed implementations, at times t = 600 s, 4200 s and 7200 s. At the upstream edge of the step the two methodologies predict the same erosion both qualitative and quantitatively independently of the time considered. Differences in behaviour appear at the downstream edge of the step. When using the upwind implementation, after some time instabilities in the shape of the bed appear just downstream of the sand step. These instabilities are due numerical effects and have not physical sense. On the other hand, the bed elevation resulting of applying the upwind & downwind implementation is smooth during the whole simulation also downstream of the step.

As is shown in Figure 8, at instant 600 s there is a change of regime, being the Froude number greater than one. The bed elevation calculated with the two methodologies is almost identical until this time. The effect of using the upwind & downwind implementation is evident in Figure 9 and Figure 10, where it can be seen that no instabilities appear either in bed elevation or in Froude number.

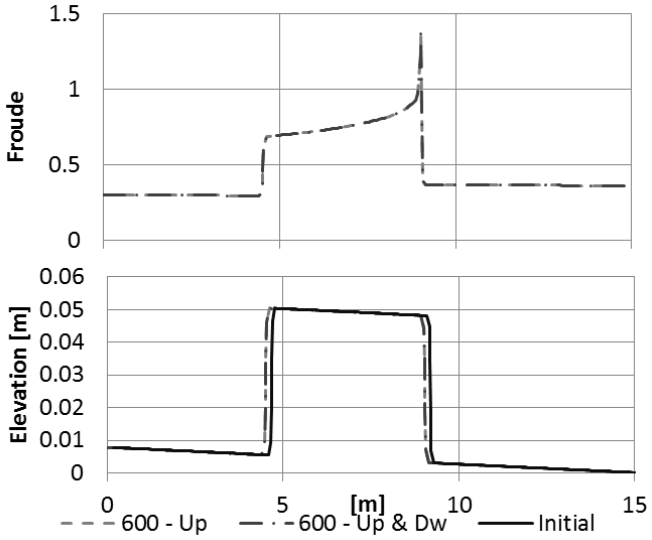

Figure 8: Bed elevation and Froude number evolutions after 600 s of simulation. Comparison between the two implementations.

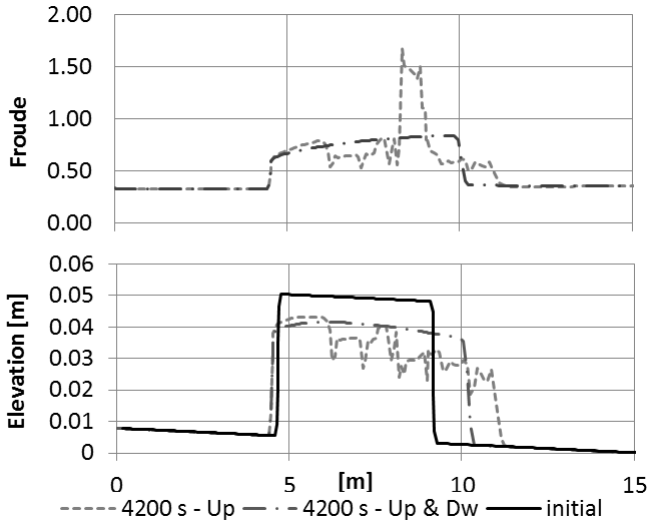

Figure 9: Bed elevation and Froude number evolutions after 4200 s of simulation. Comparison between the two implementations.

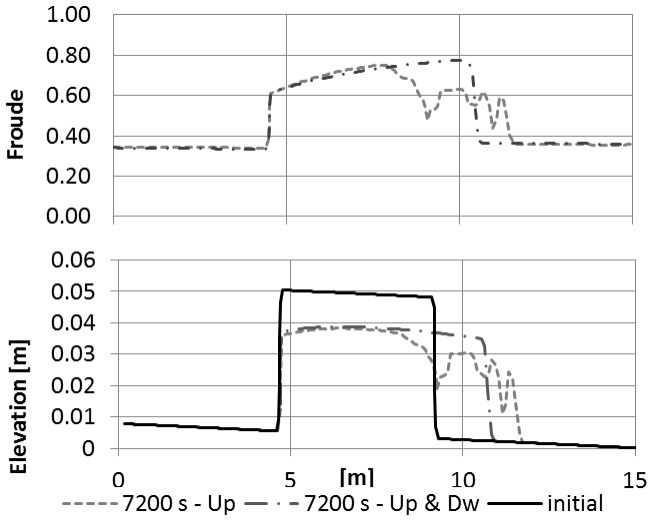

Figure 10: Bed elevation and Froude number evolutions after 7200 s of simulation. Comparison between the two implementations.

4.3 *Channel with trench and erodible reach*

In this test case a channel that can be used as benchmark for sediment transport over non erodible bottoms is proposed. It consists of a rectangular channel of 4.1 km length, 50 m wide, a slope i = 0.0001 and a Manning coefficient n = 0.03, divided in five reaches. The first four reaches are of 1 km of length. The first and third reaches are non-erodible, the second has a non-erodible layer 1 m below the initial bed, the forth has an unlimited thickness of sediment, and the last reach, of 100 m length, has also a non- erodible layer 1 m below the initial bottom (Figure 11). Uniform sediment of 2 mm of diameter and a porosity of 0.4 is used. The discharge is 1000 m^3/s, and at the downstream end there is critical depth. With this configuration the regime is mainly subcritical but at the upstream end of the fourth reach a supercritical flow with a downstream hydraulic jump is developed as the erosion process takes place. This flow regime changes are also of interest for a test case.

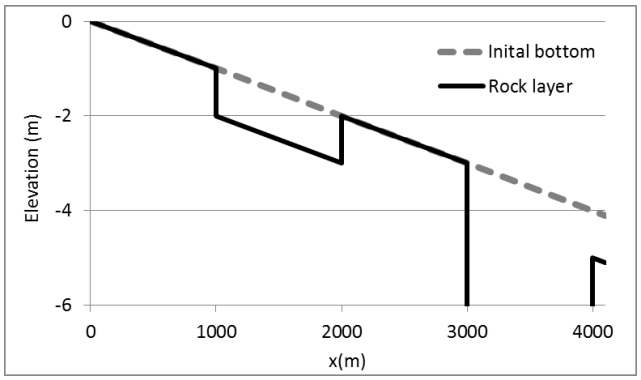

Figure 11: Chanel with non-erodible layer.

Results of two different simulations are presented:

1. No solid discharge upstream
2. Constant solid discharge of 0.0007 $m^3/s/m$

This last solid discharge value is slightly below the bedload capacity at the inlet. In both cases the Mayer-Peter & Müller formula (2) was used.

The simulations were run without sediment transport for an initial period of 1 h and then for a period of 140 days with sediments. The results of the simulations show that in both cases the first trench is eroded until no sediment is left in it, while the second erodible reach is eroded to different depths depending on if there is or there is not sediment transport upstream. In Figure 12 and Figure 14 the evolution of the channel bed is shown for both cases, together with the water surface at the final instant. It can be seen that the rock layer position is reached in the trench and at the downstream end. In Figure 13 the temporal evolution of erosion at the upstream point of the second trench is shown. It can be seen that the bed erosion tends to a final constant value.

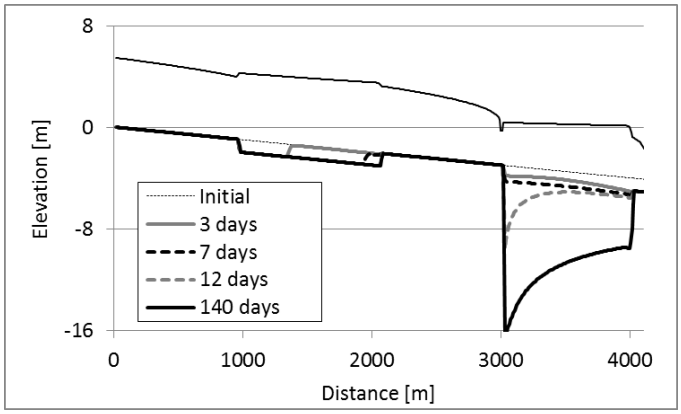

Figure 12: Bed evolution. No solid discharge upstream.

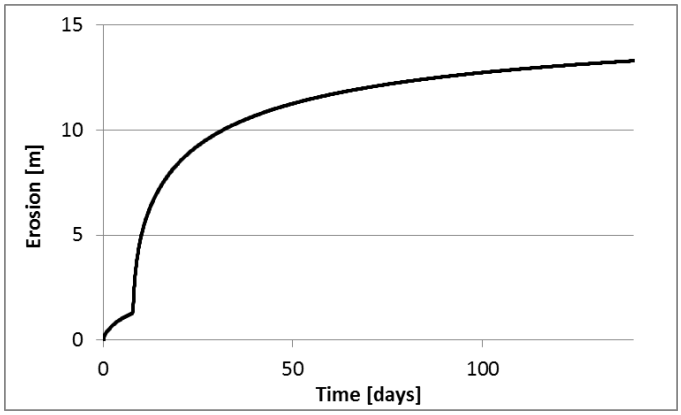

Figure 13: Erosion evolution at the upstream point of the second trench (x=3005m).

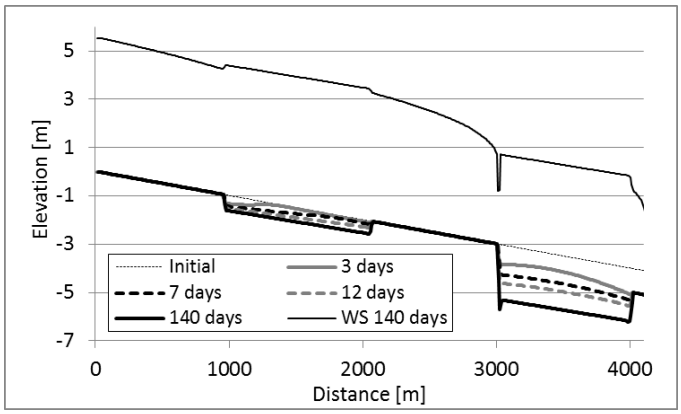

Figure 14: Bed evolution. q_s=0.0007 $m^3/s/m$ upstream.

In Figure 15 and Figure 16 the evolution of the solid discharge is represented. It can be seen that for both cases when the trench is being eroded the solid discharge increases from 0 $m^3/s/m$ to the bedload capacity. For the case of no solid discharge upstream, with 140 days of simulation the third reach is still being eroded, while for the case with bedload at the inlet, the final state is a constant solid discharge along the whole channel equal to the upstream value.

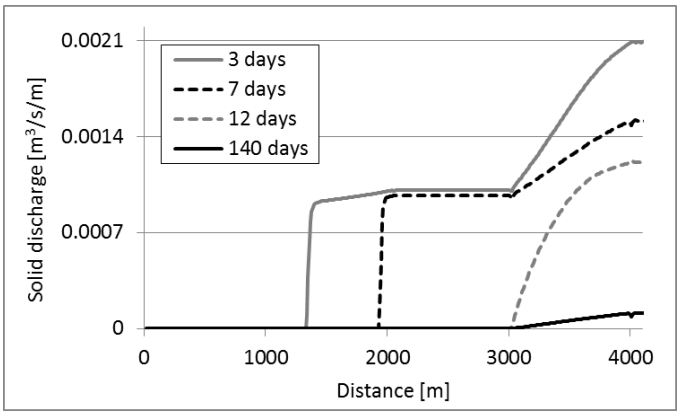

Figure 15: Solid discharge. No solid discharge upstream.

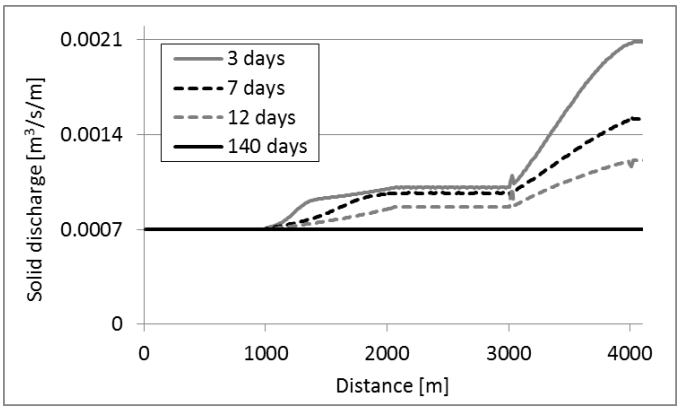

Figure 16: Solid discharge. q_s=0.0007 m^3/s/m upstream.

5 CONCLUSIONS

A bedload transport module has been implemented into a pre-existing model based on the resolution of the 2D-SWE using the Finite Volume Method. The Roe Scheme has been used for the hydrodynamic equations. We have intentionally avoided applying this scheme to the full morphodynamic (SWE + Exner) equations, because of the difficulties to use it with the commonly used bedload transport formulas in engineering. The difficulties arise when trying to obtain the Jacobian matrix, its eigenvectors and eigenvalues. The complexity of such approach with respect to the one presented here can be seen in Murillo (2010). A simple non-centred scheme has been used for the sediment continuity equation, using the sediment wave direction and not the water flow for the upwinding. The scheme, as shown in section 4.2 (Figure 10), has proved to be robust in subcritical, supercritical and mixed flows, with no spurious oscillations or instabilities that take place with other common formulations. Three different test cases have been used for verification.

The first is one of the most relevant benchmarks for sediment transport modelling: the conical sand dune, in which there is a deep interaction between the liquid flow field and the resulting bed morphology. Not only the expected star shape pattern, but also a quite accurate angle of spread is reached.

The second test proved the capability of the method to avoid instabilities when not only water flow direction is considered, but also the solid discharge celerity.

With the same intention of developing an efficient tool to be applied in engineering problems, a method to deal with a layer of non-erodible material in the river bed has been proposed and verified. The method uses a predictor-corrector scheme for the estimation of the solid discharges at finite volume intercells. If the final river bed at every time step is above the non-erodible layer, the corrector step is no needed and a direct estimation of bedload and river bed position is performed. As shown with the third test case, with the proposed method the bedload discharge can be estimated as well as erosions or deposits.

6 ACKNOWLEDGEMENTS

This work was partially founded by a PhD Grant of the Universitat Politècnica de Catalunya (UPC-Barcelona Tech).

7 REFERENCES

Benkhaldoun, F., Elmahi, I., Sari, S., and Seaid, M., 2013. An unstructured finite-volume method for coupled models of suspended sediment and bed load transport in shallow-water flows. *International Journal for Numerical Methods in Fluids*, 72 (9), 967–993.

Benkhaldoun, F., Sahmim, S., and Seaïd, M., 2009. A two-dimensional finite volume morphodynamic model on unstructured triangular grids. *International Journal for Numerical Methods in Fluids*, 63 (11), 1296–1327.

Castro Díaz, M.J., Fernández-Nieto, E.D., Ferreiro, A.M., and Parés, C., 2009. Two-dimensional sediment transport models in shallow water equations. A second order finite volume approach on unstructured meshes. *Computer Methods in Applied Mechanics and Engineering*, 198 (33-36), 2520–2538.

Grass, A.J., 1981. *Sediment Transport by Waves and Currents - Report N°: FL29*. London: SERC London Centre for Marine Technology.

Hervouet, J., Machet, C., and Villaret, C., 2003. Calcul des évolutions sédimentaires : le traitement des fonds rigides. *Revue européenne des éléments finis*, 12 (2-3), 221–234.

Hudson, J., 2001. Numerical Techniques for Morphodynamic Modelling. *PhD Thesis*. University of Reading.

Murillo, J. and García-Navarro, P., 2010. An Exner-based coupled model for two-dimensional transient flow over erodible bed. *Journal of Computational Physics*, 229 (23), 8704–8732.

Van Rijn, L.C., 1984. Sediment Transport, Part I: Bed Load Transport. *Journal of Hydraulic Engineering*, 110 (10), 1431–1456.

Rulot, F. and Dewals, B., 2012. Modelling sediment transport over partially non-erodible bottoms. *International Journal for Numerical Methods in Fluids*, 70, 186–199.

Serrano-Pacheco, A., Murillo, J., and Garcia-Navarro, P., 2012. Finite volumes for 2D shallow-water flow with bed- load transport on unstructured grids Finite volumes for 2D shallow-water flow with bed-load transport on unstructured grids. *Journal of Hydraulic Research*, 50 (2), 37–41.

Struiksma, N., 1999. Mathematical model of bedload transport over non-erodible layers. *In*: *IAHR symposium on River, Coastal and Estuarine Morphodynamics (RCEM)*. Genova, 89–98.

De Vriend, H.J., 1987. 2DH mathematical modelling of morphological evolutions in shallow water. *Coastal Engineering*, 11 (1), 1–27.

Wong, M. and Parker, G., 2006. Reanalysis and Correction of Bed-Load Relation of Meyer-Peter and Müller Using Their Own Database. *Journal of Hydraulic Engineering*, 132 (11), 1159–1168.